Synthesis, Characterization, and Metal Ion Uptake Studies of Chelating Resins Derived from Formaldehyde/Furfuraldehyde Condensed Phenolic Schiff Base of 4,4′-Diaminodiphenylmethane and *o*-Hydroxyacetophenone

S. Samal,[1] S. Acharya,[1] R. K. Dey,[2] A. R. Ray[3]

[1]*Department of Chemistry, Ravenshaw College, Cuttack-753003, India*
[2]*Department of Chemistry, Engineering College, Parlakhemundi-761211, India*
[3]*CBME, IIT, Hauz Khas, New Delhi-110016, India*

Received 22 October 2001; revised 25 March 2002; accepted 27 March 2002

ABSTRACT: The synthesis, characterization, and metal ion uptake studies of two chelating resins with multiple functional groups are reported. The chelating resins were synthesized by condensing a phenolic Schiff base derived from 4,4′-diaminodiphenylmethane and *o*-hydroxyacetophenone with formaldehyde or furfuraldehyde. The resins readily absorbed transition metal ions, such as Cu^{2+} and Ni^{2+}, from dilute aqueous solutions. The Schiff base, resins, and metal polychelates were characterized by various instrumental techniques, such as elemental-analysis, ultraviolet–visible spectroscopy proton and carbon-13 nuclear magnetic resonance spectroscopy (^{1}H-NMR and ^{13}C-NMR, respectively), X-ray diffraction (XRD), and thermogravimetric–differential thermogravimetric analyses (TG–DTG). The ^{1}H-NMR and ^{13}C-NMR studies were used to determine the sites for aldehyde condensation with the phenolic moiety. Fourier transform infrared data provided evidence for metal–ligand bonding. Thermogravimetric analysis was employed to compare the relative thermal stabilities of the resins and the polychelates. The TG data were fitted into different models and subjected to computational analysis to calculate the kinetic parameters. The XRD data indicate that the incorporation of metal ion into the resin matrix significantly enhanced the degree of crystallinity of the material. The extent of metal-ion loading into the resins was studied in competitive and noncompetitive conditions, varying the time of contact, metal ion concentrations, and pH of the reaction medium in a suitable buffer medium. The furfuraldehyde-condensed resin was more effective in removing metal ions than the formaldehyde-condensed resins. The resins were selective for Cu^{2+}, resulting in separation of Cu^{2+} and Ni^{2+} from the mixture at pH 5.89. © 2003 Wiley Periodicals, Inc. J Appl Polym Sci 88: 570–581, 2003

Key words: Schiff base; chelating resin; metal uptake

INTRODUCTION

Chelate-forming polymeric ligands, which are characterized by reactive functional groups containing O, N, S, and P donor atoms and are capable of coordinating to different transition metal ions, have been extensively studied.[1] These materials most often show preferential selectivity towards certain metal ions like Cu(II), Ni(II), etc., thus facilitating their use for preconcentration and separation of trace metal ions from saline and nonsaline water. Parmer and co-workers[2] synthesized resacetophnone–formaldehyde resin in acidic medium and studied its chelation properties. Zigon et al.[3,4] synthesized resorcinol–formaldehyde–crotonaldehyde resin in different media and characterized the polymer. Moyer and Fritz[5] condensed *m*-phenylenediaminetetraacetic acid with resorcinol and formaldehyde to get a resin containing two iminodiacetic acid functional groups anchored to a benzene ring and used these resins for separating Co^{2+} from Ni^{2+} in a gravity flow column. Dumont and co-workers[6] synthesized a number of resins by polycondensation of formaldehyde with phenol, resorcinol, catechol, and phloroglucinol in alkaline media and used these resins in the selective extraction of cesium from alkaline-leaching solutions of spent catalysts. Samant and Mishra[7] used resorcinol–formaldehyde resin for removal of cesium from nuclear waste. Condensation polymerization of phenol–formaldehyde–piperazine resulted in a resin selective for Cu^{2+}.[8,9]

Schiff bases with multidentate coordination sites are known to readily form complexes with transition metal ions.[10] When present in a polymer matrix, Schiff bases are expected to show affinity and selectivity towards transition metal ions at an appropriate pH. We have synthesized phenol–formaldehyde-type

Correspondence to: R. K. Dey (rkdey@rediffmail.com).

Journal of Applied Polymer Science, Vol. 88, 570–581 (2003)

polymers by condensing the phenolic Schiff bases with formaldehyde and furfuraldehyde and used these polymers for the separation of metal ions.[11] The present communication deals with the synthesis of resins of formaldehyde (HCHO)- and furfuraldehyde (FFD)-condensed phenolic Schiff bases of 4,4′-diaminodiphenylmethane (DDM) with o-hydroxyacetophenone (*o*-HAP), and the characterization and study of the metal ion uptake behavior of the resins towards Cu^{2+} and Ni^{2+}.

EXPERIMENTAL

Reagent

The following starting materials were used as received: *o*-hydroxyacetophenone(*o*-HAP), 4,4′-diaminodiphenylmethane (DDM) (Merck, Germany), the sulfate and nitrate salts of Cu^{2+} and Ni^{2+}, respectively, and formaldehyde (HCHO), furfuraldehyde (FFD), and all other chemicals and solvents (AnalarR/GR grade, Merck/BDH, India). The buffers used to control the pH of the solution were acetic acid–sodium acetate (pH 3.42–5.89), disodium hydrogen phosphate–potassium dihydrogen phosphate (pH 5–8), and ammonium hydroxide–ammonium chloride (pH 8–10).

Preparation of Schiff base

The Schiff base monomer *o*-HAP–DDM was synthesized by reacting 1.96 g (0.01 mol) of DDM dissolved in 10 mL of methanol with 2.72 g (0.02 mol) of *o*-HAP in the presence of 0.5 g of anhydrous sodium acetate. The mixture was refluxed for 1 h at 70°C, poured into ice-cold water, and allowed to stand for 30 min. The precipitated solids were filtered off, washed repeatedly in demineralized water, and recrystallized from ethanol. The Schiff base (*o*-HAP–DDM) was isolated as a light yellow crystalline solid; ^{1}H-NMR (300 MHz, $DMSOd_6$, δ) 2.62, 3.58, 6.52–7.87 (m); FTIR (KBr pellet) $\tilde{\nu}_{max}$ (cm^{-1}) 3379.1, 1608.5, 1573.8, 1502.4, 1211.2, 748.3; Anal. Calcd. C, 80.086; H, 6.031; N, 6.44; found; C, 80.1; H 6.02; N 6.42.

Preparation of resins

The Schiff base monomers (1 g, 0.0023 mol) were suspended in 20 mL of water at 40°C and dissolved in a minimum volume of NaOH (1 M). Paraformaldehyde/FFD in a 1 : 2 molar ratio was added, and the mixture was refluxed in an oil bath at 120–130°C for 2 h. The insoluble resins were filtered off, washed repeatedly with distilled water, and dried at 70°C. The yield of both the resins, *o*-HAP–DDM–HCHO and *o*-HAP–DDM–FFD exceeded 70%. The dried resins were powdered, seived (100 mesh, ASTM), and suspended over water at pH 4 overnight. These resins were filtered off, washed in a large excess of water followed by methanol, and dried in a vacuum at 70°C. *o*-HAP was also condensed with HCHO or FFD, yielding *o*-HAP–HCHO and *o*-HAP–FFD resins, respectively.

The IR and ^{1}H-NMR spectra of these resins were compared with those of the Schiff base resins to find out if the Schiff base monomers suffered hydrolysis under the reaction conditions used for polymerization; *o*-HAP–DDM–HCHO: ^{1}H-NMR (300 MHz, $DMSOd_6$/$CDCl_3$, δ) 3.36–4.63, 6.54–7.86; FTIR (KBr pellet) $\tilde{\nu}_{max}$ (cm^{-1}) 3365.6, 2906.5, 1616.2, and 1514; Anal. Found: C, 69.34; H, 4.35; N, 4.67; *o*-HAP–DDM–FFD: ^{13}C-NMR (75 MHz, $DMSOd_6$; ppm) 158.3; 71.6; FTIR (KBr pellet) $\tilde{\nu}_{max}$ (cm^{-1}) 3200, 1641.3, 1581.5, 1548.3, 1512.1, 1467.7, 1209.3, and 748.3, Anal. Found: C, 61.89; H, 4.55; N, 2.78.

Preparation of the polychelates

To 100 mg of dry resin (100 mesh, ASTM) suspended over methanol was added 10 mL of metal salt (0.15 M) in water. The mixture was stirred for 2 h at 40°C. The resin was filtered off, washed in distilled water followed by petroleum ether, and dried in vacuum at 70°C; *o*-HAP–DDM–HCHO–Cu(II): FTIR (KBr pellet) $\tilde{\nu}_{max}$ (cm^{-1}) 3415.7, 2923.9, 1616.1, 1508.2, 1193.9, 505.3, 449.4; Anal. Found C, 54.3; H, 3.34; N, 3.21; *o*-HAP–DDM–FFD–Cu(II): FTIR (KBr pellet) $\bar{\upsilon}$(cm^{-1}) 3375.2, 1604.7, 1548.7, 1512.1, 1213.1, 752.2, 594, 511.1.

Metal ion uptake studies

The metal ion uptake behavior of the resins was determined by the batch method. A suspension of the resin in a metal solution of known volume and concentration was agitated for a definite time period over a hot plate/magnetic stirrer. The pH of the solution was adjusted using a suitable buffer. The resin was filtered off and thoroughly washed in demineralized water. The metal ion content in the filtrate and the washings were collected, and quantitative determination of the metal ion concentration was done by the neocuproin method for Cu(II), dimethylglyoxime method for Ni(II).[12] The percentage of metal ion adsorbed by the resins was calculated using the following relation:

$$\text{Metal ion uptake (\%)} = W_i - W_f/W_i \qquad (1)$$

where W_i is the amount (μg) of the metal ion initially present in solution and W_f is the amount (μg) of rotation remaining in the solution after adsorption.

TABLE I
Color and Solubility

Compound	Color	Solubility in different solvents[a]						
		H_2O	CH_3OH	CCl_4	$CHCl_3$	DMF	DMSO	THF
o-HAP-HCHO	Yellow	−	−	±	±	+	+	+
o-HAP-FFD	Black	−	−	±	±	+	+	+
o-HAP-DDM	Yellow	−	±	+	+	+	+	+
o-HAP-DDM-HCHO	Yellow	−	−	−	−	−	−	−
o-HAP-DDM-HCHO-Cu(II)	Yellowish blue	−	−	−	−	−	−	−
o-HAP-DDM-HCHO-Ni(II)	Yellowish Green	−	−	−	−	−	−	−
o-HAP-DDM-FFD	Black	−	−	±	±	+	+	+
o-HAP-DDM-FFD-Cu(II)	Grey	−	−	±	±	+	+	+
o-HAP-DDM-FFD-Ni(II)	Grey	−	−	±	±	+	+	+

[a] (+) Soluble, (±) Partially soluble, (−) Insoluble

Measurements

The elemental analysis was carried out with a Carlo Erba 1108 elemental analyzer. The FTIR spectra were recorded with a Perkin Elmer spectrophotometer model 1800 in the range 4000–200 cm^{-1} in the KBr phase. The ^{1}H-NMR spectra were recorded in $DMSOd_6$ or $DMSOd_6/CDCl_3$ with 300/400 MHz FT ^{1}H-NMR (Bruker DRX 300/Bruker WM400) instruments. The proton-decoupled ^{13}C-NMR spectra were recorded with a VXR-300-S-Varian Supercon NMR spectrophotometer operating at 75 MHz. The TG behavior of the materials was recorded with a Du-Pont 9900 thermogravimetry analyzer at a heating rate of 10°C/min in a nitrogen atmosphere. The XRD study was performed with a PW 1820 diffractometer using a Cu X-ray tube operating at 40 kV and 30 mA in the 2θ range 4–35°. The estimation of the metal ion concentration in the dilute aqueous solutions was made with a Systronic Digital spectrophotometer model 116, and the pH of the solutions was measured in a Systronics Digital pH meter model 335.

RESULTS AND DISCUSSION

Solubility

The freshly prepared resin (100 mesh, 10 mg) was suspended over 5 mL of the chosen solvent at room temperature (27°C), and the solubility of the resin was checked after 24 h (Table I). Both the *o*-HAP–DDM–HCHO and *o*-HAP–DDM–FFD resins were completely insoluble in water. The formaldehyde-condensed resin, *o*-HAP–DDM–HCHO, was insoluble in select organic solvents, which could be attributed to the increase in molecular weight of the resin due to crosslinking. In the network structure, the various structural units are connected through —C H_2— groups, leading to a rigid structure. On the other hand, the furfuraldehyde-condensed resin, *o*-HAP–DDM–FFD, was partially soluble in CCl_4 and $CHCl_3$, and completely soluble in DMSO and THF. This improvement in solubility is due to the presence of the furan ring on the bridging methylene carbon, which presumbly led to inefficient molecular packing and, consequently, easy swelling of the polymer. The solubility of the resin studied over a period of time decreased steadily. This decrease could be ascribed to curing of resins, resulting in crosslinking, and consequently an increase in molecular weight. Curing is known to be a characteristic of the phenol–formaldehyde resin.[13] The decrease in solubility of the polychelates could be due to the alteration in the polymer polarity and intrapolymer crosslinking,[9] as well as increase in crystallinity.[14]

Elemental analysis

The elemental analysis (C, H, N) data of the Schiff base agrees closely with the theoretical values. The Schiff base unit could be joined up through ortho–ortho, ortho–para, and para–para linkages. The solubility characteristics data indicate that the formaldehyde-condensed resin is more crosslinked than the furfuraldehyde-condensed resin. A comparison of the theoretical and experimental elemental analysis data of the repeating units indicates some discrepancy, which can be attributed to the presence of a large number of solvent molecules, mostly water, attached to the polymer matrix through hydrogen bonding. A similar discrepancy between theoretical and calculated values for C, H, and N was reported by several authors[15,16] and attributed to the strong tendency of the ligands for taking up moisture.

Spectral studies

FTIR study

The FTIR spectra of the Schiff base, the resins, and the polychelates are shown in Figure 1. The spectra of *o*-HAP–HCHO and *o*-HAP–FFD show strong C═O

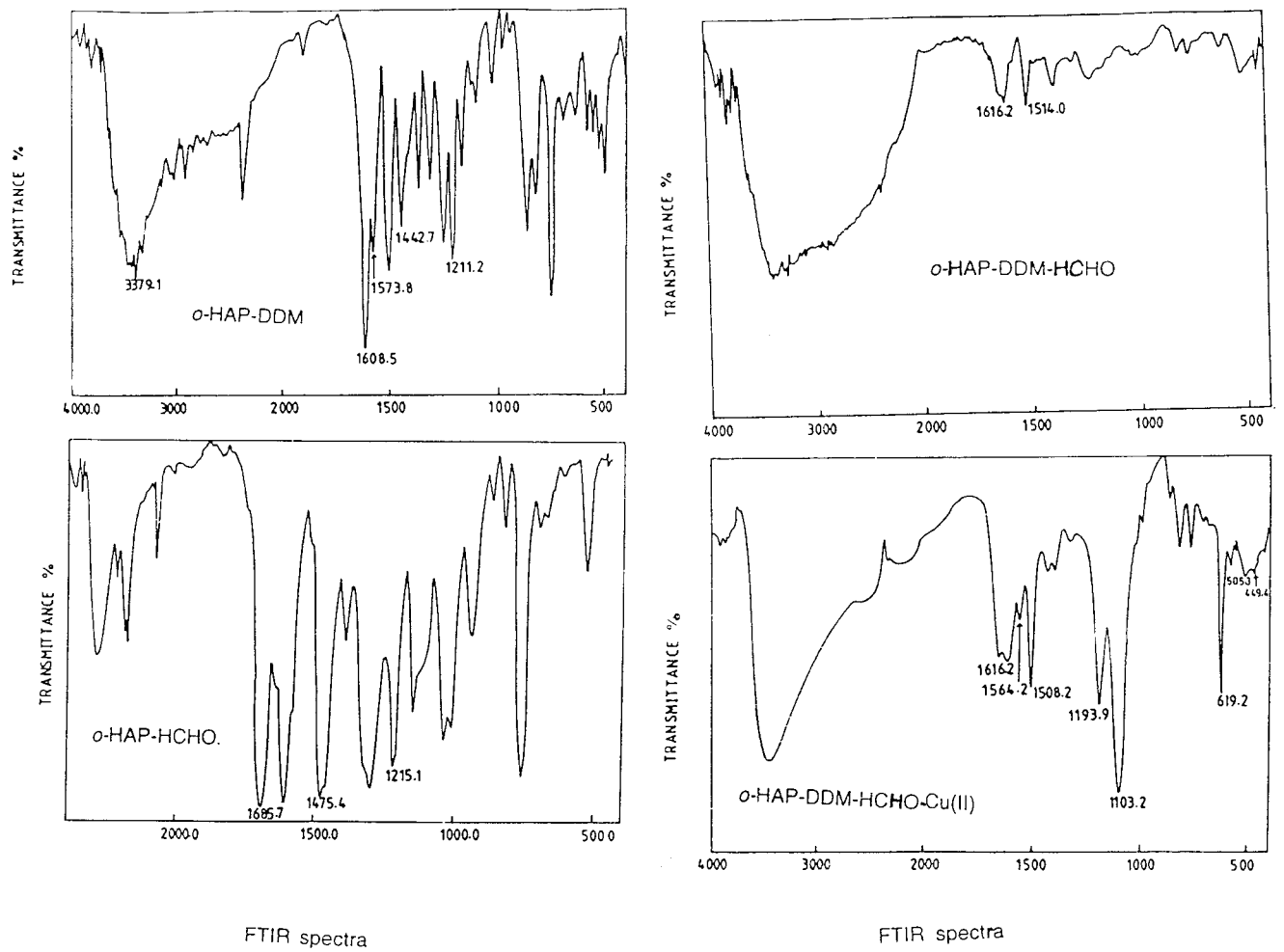

Figure 1 FTIR spectra of *o*-HAP–DDM *o*-HAP–HCHO, *o*-HAP–DDM–HCHO, and *o*-HAP–DDM–HCHO–Cu(II).

absorption at 1685.7 and 1700 cm^{-1}, respectively, which is absent in the *o*-HAP–DDM–HCHO and *o*-HAP–DDM–FFD resins, indicating that the Schiff base did not undergo hydrolysis under the reaction conditions used for condensation polymerization. In the Schiff base *o*-HAP–DDM, the C═N stretch appears at 1608.5 cm^{-1}, the phenolic O—H registers at 1211.2 cm^{-1}, and the C═C absorptions are at 1573.8, 1502.4, and 1442.2 cm^{-1}. Most of the peaks in the fingerprint region are sharp and well resolved. However, on condensation with HCHO or FFD, most of the aforementioned characteristic bands of the Schiff base either are diminished in intensity or vanish. The resin *o*-HAP–DDM–HCHO shows C═N absorption at 1616.2 cm^{-1}.[17] The hydrogen bonded O—H stretch appears as a broad band at 3365.6 cm^{-1}. The aliphatic C—H stretch for methylene and/or methylol groups generated on formaldehyde condensation is registered at 2906.5 cm^{-1} as a weak band. In the furfuraldehyde-condensed Schiff base polymer *o*-HAP–DDM–FFD, the C═N stretch is observed at 1641.3 cm^{-1}, the phenolic O—H bond is at 1209.3 cm^{-1}, and the C═C stretches are at 1581.5, 1548.7, 1512.1, and 1467.7 cm^{-1}.

The C═N stretch for the *o*-HAP–DDM–HCHO–Cu(II) polychelate does not register any shift from its original position in the resin. The Ph—O absorption is at 1193.9 cm^{-1}. The C═C stretch registers a shift from 1514 cm^{-1} in the resin to 1508.2 cm^{-1} in the polychelate. However, in the case of the *o*-HAP–DDM–FFD–Cu(II) polychelate, the C═N registers a significant shift to 1604.7 cm^{-1}, which is towards a lower frequency region compared with its original position in the resin of 1641.3 cm^{-1}. The Ph—O absorption registers a shift of 4 cm^{-1} towards a higher frequency region in comparison with the corresponding resin. Several authors have made similar observations.[18–20] In addition, in the FTIR spectra of both the polychelates, absorptions at 594–505.3 and 511.1–499.4 cm^{-1} are observed and assigned to the M—O and M—N bonds, respectively. Ueno and Martell[10,a] have made extensive band assignments for the metal chelate compounds of bis-acetylacetone–ethylenediimine and bis-salicylaldehyde–ethylenediimine and have assigned the metal–ligand stretching vibrations in these Schiff base complexes to the range 640–500 cm^{-1} for the M—O and 580–430 cm^{-1} for the M—N bonds.

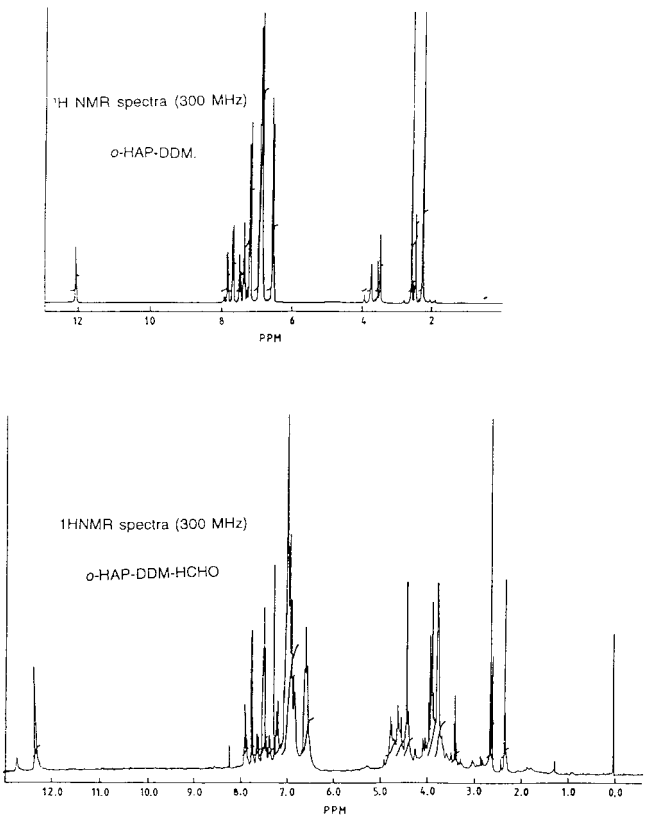

Figure 2 ^{1}H-NMR spectra of *o*-HAP–DDM and *o*-HAP–DDM–HCHO.

In addition to the phenolic oxygen and aldimine nitrogen binding the metal ion, there is evidence that the counterion SO_4^{2-} from $CuSO_4$ used to synthesize *o*-HAP–DDM–HCHO–Cu(II) and *o*-HAP–DDM–FFD–Cu(II) acts as a bridging group between metal ions (Cu^{2+}—O—SO_2—O —Cu^{2+}). This conclusion is based on the characteristic modes of sulfate group vibrations observed at 1193.9, 1103.2, and 619.2 and 1153.3, 1099.3, and 1043.5 cm^{-1} for *o*-HAP–DDM–HCHO–Cu(II) and *o*-HAP–DDM–FFD–Cu(II), respectively. Nakamato et al.[21] studied bridged sulfate complexes of Co(II) and reported similar observations.

In the case of Ni(II) polychelates, the M—O and M—N bands are not sharp and no shift is noticed in the phenolic C—O and C═N absorptions. This observation indicates a lower preference of the resin for Ni^{2+} than for Cu^{2+}. The Ni(II) polychelates also show a strong absorption band at 1400 cm^{-1}, which is characteristics of a free NO_3^- from $Ni(NO_3)_2$ used for polychelate synthesis.[22] Both Cu(II) and Ni(II) polychelates also show absorptions at ~ 3400, 900, and 400 cm^{-1}, indicating the presence of coordinating as well as lattice water.[23]

^{1}H-NMR spectra

The ^{1}H-NMR spectra of Schiff base, resins, and the polychelates are shown in Figure 2. The methyl protons of the o-HAP moiety in the *o*-HAP–DDM Schiff base are observed at 2.62 ppm. The methylene proton of the DDM moiety appears at 3.58 ppm. The peaks in the aromatic region are seen as a set of multiplets in the range 6.52–7.87 ppm. The phenolic O—H proton is at 12.09 ppm.[24] The formaldehyde-condensed resins *o*-HAP–HCHO and *o*-HAP–DDM–HCHO have a number of additional peaks in the form of complex multiplets in the range 3.36–4.73 ppm. These peaks are ascribed to the bridging methylene (ϕ—CH_2—ϕ) and the methylene groups of terminal methylol (ϕ—CH_2OH) functions.[25] The aromatic ring protons appear as broad and overlapping multiplets in the range 6.54—7.86 ppm.

The furfuraldehyde-condensed resins *o*-HAP–FFD and *o*-HAP–DDM–FFD do not show a bridging methylene proton. Such a proton in the triphenylmethane-type structure is assigned in the range 5.5–6 ppm,[26] and Dimitrov et al.[27] also noticed the methylene proton in this range. The appearance of this proton in the relatively weak field is attributed to the higher deshielding effect associated with the triphenylmethane-type structure.

In the complex *o*-HAP–DDM–HCHO–Cu(II), the intensity of the O—H proton peak is sharply reduced. The aromatic ring protons that are seen in the range 6.9–8.12 ppm become broad and less intense in comparison with the corresponding resin. This effect may be due to the drifting of ring electrons towards the metal ion following complexation to metal ion.

Similarly, in the case of *o*-HAP–DDM–FFD–Cu(II), the O—H proton appears at 12.3 ppm with reduced intensity. The intensity of the water peak is very high, indicating the presence of a large excess of water in the polychelate either in the lattice or in the coordinated form. The aromatic ring protons that are in the range 6.29–8.09 ppm become broad and less intense.

^{13}C-NMR spectra

The ^{13}C-NMR spectra of *o*-HAP–DDM and its furfuraldehyde-condensed resin are given in Figure 3. The *o*-HAP–DDM–FFD resin spectrum has a number of peaks between 109.9 and 161.3 ppm. The peak at 158.3 ppm is ascribed to the carbon attached to phenolic O—H group. A sharp peak at 71.6 ppm is assigned to the —CH(OH)—terminal function, which was generated due to the reaction of the phenolic moiety with furfuraldehyde. Zigon et al.,[3] while studying the ^{13}C-NMR spectrum of the resorcinol–cinnamaldehyde resin, observed the —CH(OH)— signals between 65 and 72 ppm.

Thermogravimetric analyses

The TG–DTG data of the resins and the corresponding Cu(II) polychelates were analyzed to evaluate the rel-

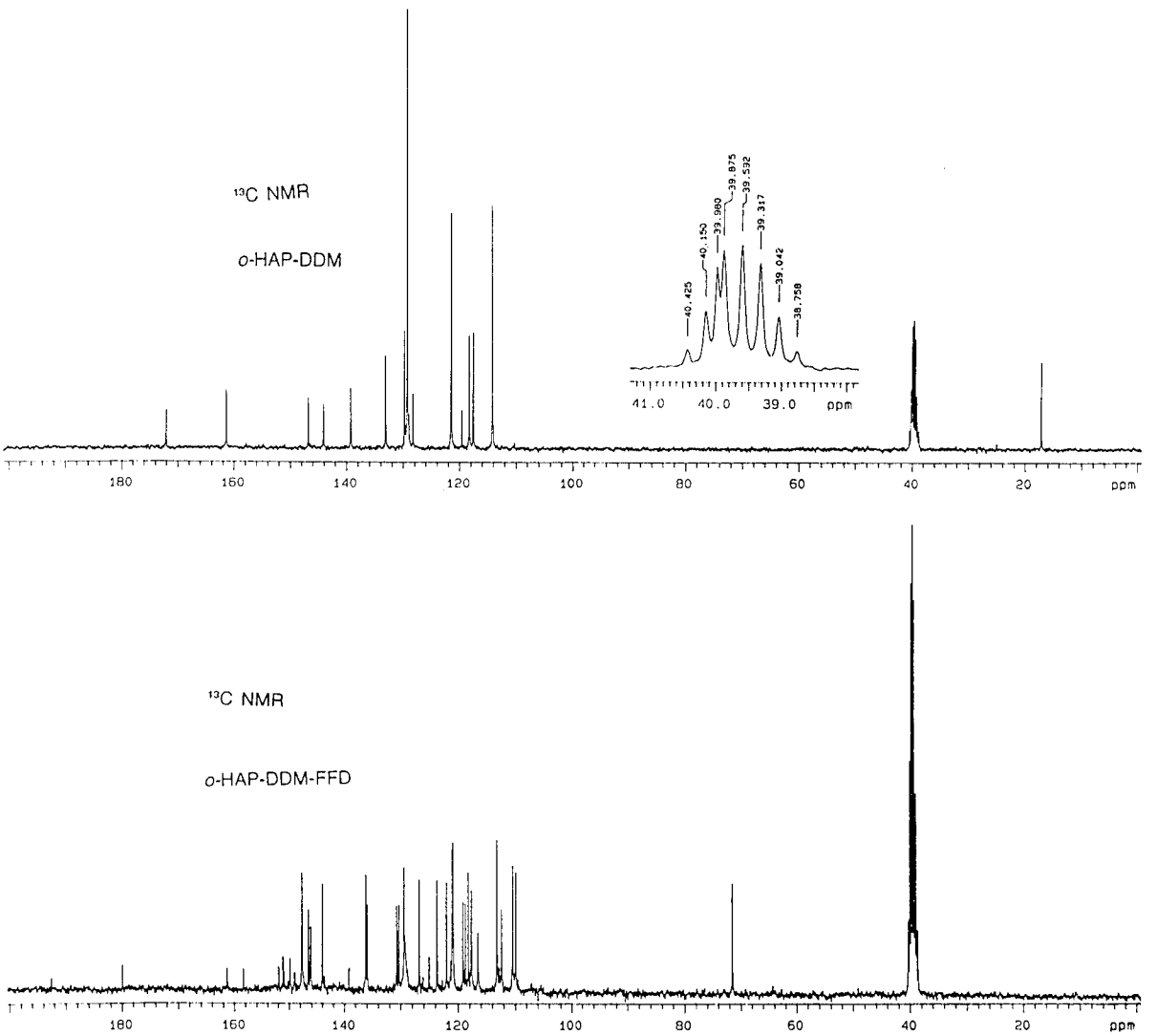

Figure 3 ^{13}C-NMR spectra of *o*-HAP–DDM and *o*-HAP–DDM–FFD.

ative thermal stability of the materials. The thermograms of the resins *o*-HAP– DDM–HCHO and *o*-HAP–DDM–FFD and those of their Cu(II) polychelates, *o*-HAP–DDM–HCHO–Cu(II) and *o*-HAP–DDM–FFD–Cu(II), are given in Figure 4, and the relevent data are furnished in Table II. The *o*-HAP–DDM–HCHO resin lost 1.12% of its weight upto 130°C whereas its Cu(II) polychelate was stable up to 170°C. Between 130 and 200°C, the resin lost 7.84% of its original weight, but the polychelate suffered negligible weight loss (1.15%). These observations indicate that the resin matrix contained loosely bound low molecular weight species, such as water, which could be easily desorbed.

Beyond 200°C, the resin lost weight in three different stages, at the rates of 0.1862, 0.1447, and 0.5757%/°C at peak decomposition temperatures of 206.86, 286.14, and 570.33°C, respectively. The rate of weight loss at peak decomposition temperature (570.33°C) was much faster than that at the earlier two stages. The temperature at which the rate of weight loss (in %/°C) was maximum, T_{max}, was 570.33°C. The char yield at 600°C was 16.59%, which decreased to 2.803% at 700°C.

In the range 200–600°C, the polychelate *o*-HAP–DDM–HCHO–Cu(II) lost 37.02% of its weight in multiple stages. The rate of weight loss was 0.291% at the T_{max} of 475.01°C. The char yield at 700°C was 55.69%. The high percentage of char yield was due to the formation of nonvolatile metal oxides.

The thermal degradation patterns of *o*-HAP–DDM–FFD and *o*-HAP–DDM–FFD–Cu(II) indicate that the resin did not loose weight up to 120°C, whereas, the polychelate was stable upto 160°C. Between 130 and 200°C, the weight loss was not significant for both the resin and the polychelate. Between 200 and 600°C, the resin lost 65.25% of its original weight at a rapid rate. The T_{max} was 550.20°C and the rate of weight loss at this temperature was 0.4247%/°C. The char residue was 9.466% at 700°C. The polychelate on the other

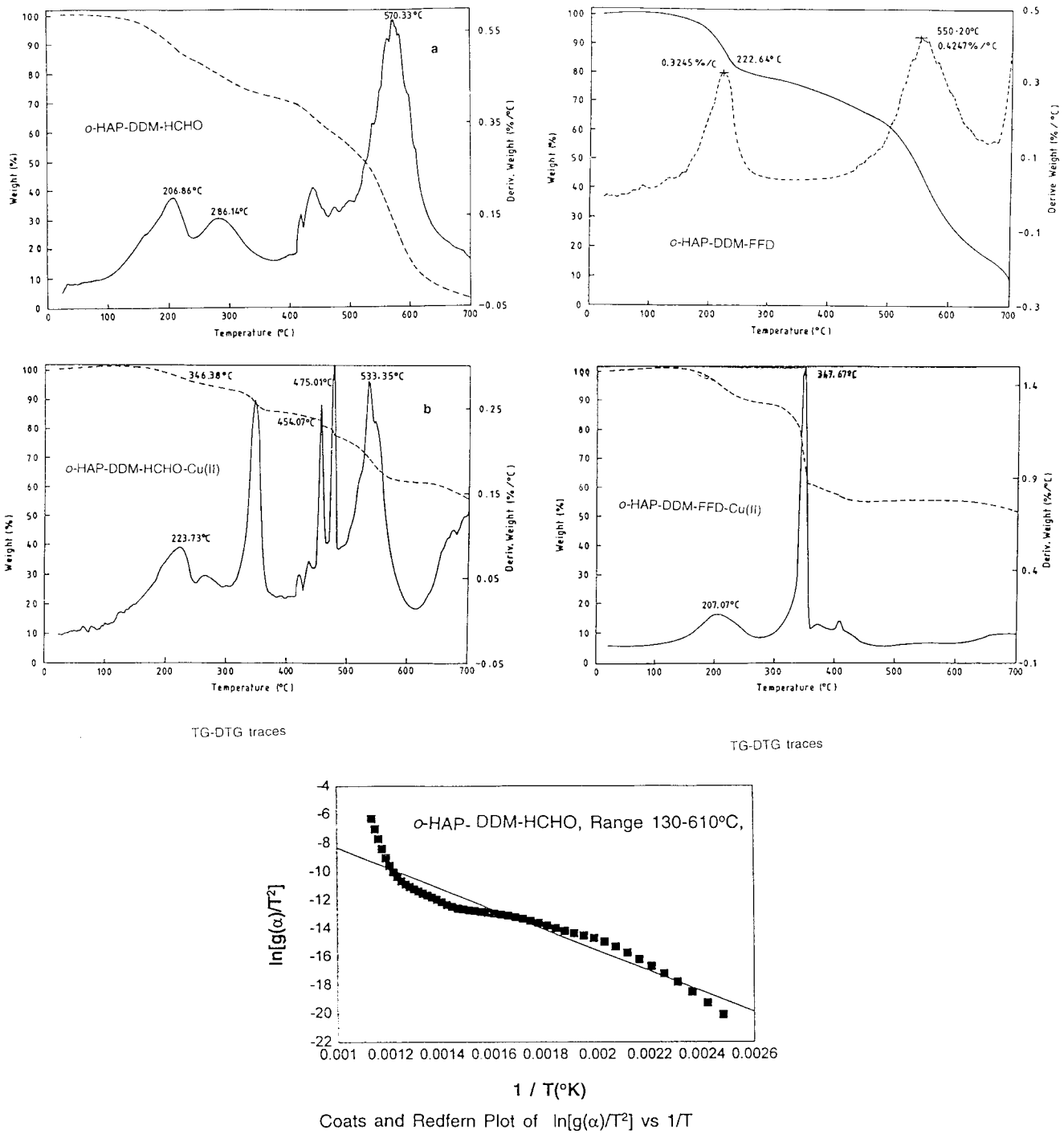

Figure 4 TG–DTG traces of *o*-HAP–DDM–HCHO, *o*-HAP–DDM–HCHO–Cu(II), *o*-HAP–DDM–FFD, and *o*-HAP–DDM–FFD–Cu(II), and Coats and Redfern plot of $\ln[g(\alpha)/T^2]$ versus $1/T$.

hand lost only 40.69% between 200 and 600°C, in two stages at rates 0.1597%/°C (207.07°C) and 1.476%/°C. The char yield was 51.98% at 700°C and ascribed to nonvolatile metal oxides. These observations show that the thermal decomposition pattern is not a clear indication of relative thermal stability. To corroborate the findings, the kinetic parameters for thermal decomposition of the resins and the polychelates were evaluated using various integral methods of Coats–Redfern (eq. 2), 28 Van Krevelen (eq. 3),[29] and Broido (eq. 4).[30]

$$\ln[g(\alpha)/T^2] = \ln[AR/\beta E(1 - 2RT/E)] - E/RT \quad (2)$$

$$\ln[g(\alpha)] = \ln[A/\beta(0.368/T_{\max}(E/RT_{\mathrm{m}} + 1)^{-1}] + (E/RT_{\max} + 1)\ln T \quad (3)$$

TABLE II
Thermogravimetric Data

Compound	Percent weight loss				Y_c(%)[a]	
	Up to 130°C	130–200°C	200–400°C	400–600°C	600°C	700°C
o-HAP-DDM-HCHO	1.12	7.84	20.95	53.5	16.59	2.803
o-HAP-DDM-HCHO-Cu(II)	0	1.15	13.8	23.22	61.83	55.69
o-HAP-DDM-FFD	0.23	6.23	20.48	44.77	28.29	9.466
o-HAP-DDM-FFD-Cu(II)	0	3.86	38.48	2.21	55.45	51.98

[a] Percentage of char yield at 600 and 700°C.

$$\ln[g(\alpha)] = \ln[A/\beta \times (R/E)T_{max}^2] - (E/R) \times 1/T \qquad (4)$$

where $\alpha = [W_o - W_f]/[W_o - W_f]$, W_o is the initial weight, W is the weight at temperature T, W_f is the final weight, β is the heating rate, T_{max} is the temperature of the maximum rate of weight loss (K), E is the activation energy (Kcal), A is the frequency factor (s^{-1}), and $g(\alpha)$ is a function of α, with the various α values depending on the mechanism of thermal decomposition.

The activation energy, E, and the frequency factor, A, were computed for the different models from the slope and the intercept of a plot of $\ln[g(\alpha)/T^2]$ versus $1/T$ for the Coats and Redfern model, a plot of $\ln[g(\alpha)]$ versus $\ln T$ for the Van Krevelen model, and a plot of $\ln[g(\alpha)]$ versus $1/T$ for the Broido model after linear regression of the data (Figure 4). The Coats and Redfern model does not involve T_{max} in the expression. This model was used to evaluate the kinetic parameters in the entire range (130–610°C). On the other hand, the Van Krevelen and Broido models make use of T_{max} in the expressions and, hence, were used to calculate the kinetic parameters for different decomposition stages using the relevant T_{max} value of each stage. The entropy of activation, ΔS (cal K^{-1} mol^{-1}) was calculated using the relation $A = (kT_{max}/h)\,(e\Delta^{S/R})$, where k is the Boltzmann constant (0.32944×10^{-23} cal K^{-1}), h is Planck's constant (1.5836×10^{-34} cal s), and R is the gas constant (1.9872 cal K^{-1} mol^{-1}).

Analysis of the activation energy data (Table III) indicates that both the resins, *o*-HAP–DDM–HCHO and *o*-HAP–DDM–FFD, were less stable than their corresponding Cu(II) polychelates. Several workers[28,29] have reported that the incorporation of metal ions into the polymer matrix increases thermal stability.

XRD study

The XRD patterns of the *o*-HAP–DDM–HCHO resin and its Cu(II) polychelate are presented in Figure 5. The resin has only one peak at 2θ 30°. The polychelate has a number of reflection planes. The most intense peak appears at 31.78° along with a number of moderately intense peaks at 25.8, 27.68, and 31.17°. This increase in number of peaks is ascribed to a significant increase in the crystallinity of the polymer following chelation with the metal ion. A comparison of the peak area indicates that the polychelate can be nearly 30 times more crystalline than the resin. However, the observed increase in the number of reflections and intensity could also be the result of an increase in electron density due to the metal ion uptake. Yang and Chen[14] reported that polymers with paraphenylene units exhibit one strong reflection at ~ 20° and weaker

TABLE III
Kinetic Parameters

Compound	Temperature range (°C)	T_{max} (°K)	Method[a]	E (kcal)	A (s^{-1})	ΔS (CalK^{-1} mol^{-1})
o-HAP-DDM-HCHO	130–610	—	CR	13.862	1.52E + 04	−41.470
		843.33	VK	6.666	2.09E + 00	−59.150
		843.33	BR	5.445	6.06E − 01	−61.608
o-HAP-DDM-HCHO-Cu(II)	130–610	—	CR	4.848	1.00E + 02	−51.220
		748.01	VK	19.115	2.61E + 05	−35.582
		748.01	BR	16.522	3.82E + 04	−39.405
o-HAP-DDM-FFD	130–610	—	CR	9.062	2.90E + 03	−44.720
		823.2	VK	9.952	1.26E + 02	−50.948
		823.2	BR	6.954	2.35E + 00	−58.866
o-HAP-DDM-FFD-Cu(II)	130–610	—	CR	23.155	1.82E + 10	−13.045
		620.67	VK	20.508	1.58E + 07	−27.053
		620.67	BR	20.740	2.85E + 07	−25.887

[a] CR, Coats–Redfern; VK, Van Krevelen; BR, Broido.

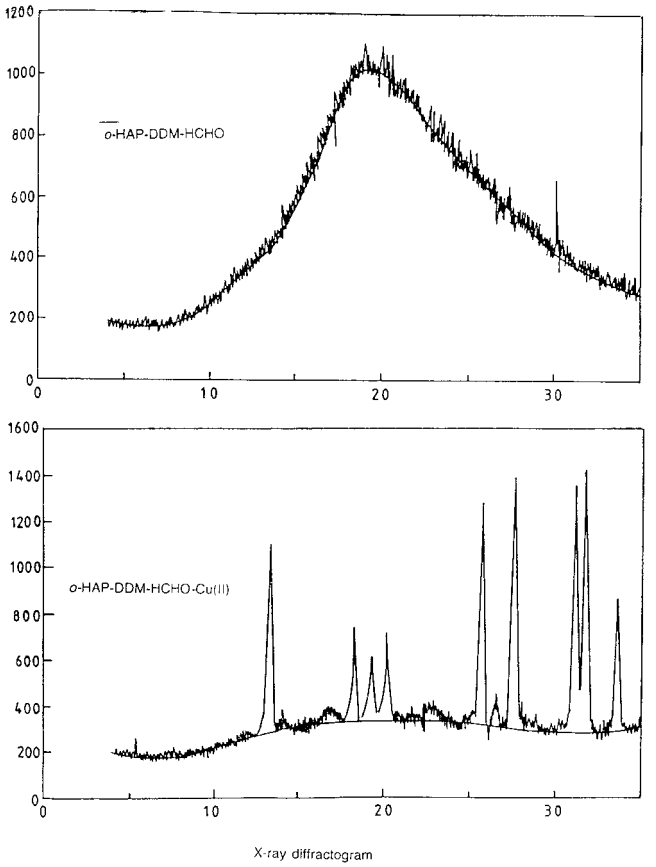

Figure 5 X-ray diffractograms of *o*-HAP–DDM–HCHO and *o*-HAP–DDM–HCHO–Cu(II).

reflections at 27°. The authors ascribed these peaks to the crystalline nature of the resin.

Structural features

The information obtained from the spectroscopic studies led us to propose a structure for the resins and Cu(II)-polychelates. The FTIR spectra of *o*-HAP–DDM–HCHO–Cu(II) indicate that the metal ion is bound to the resin matrix via coordination of phenolic oxygen and the imine nitrogen. The SO_4^{2-} ion is present as a bridging group. To account for these observations, a structure for *o*-HAP–DDM–HCHO–Cu(II) was proposed and is shown in Figure 6.

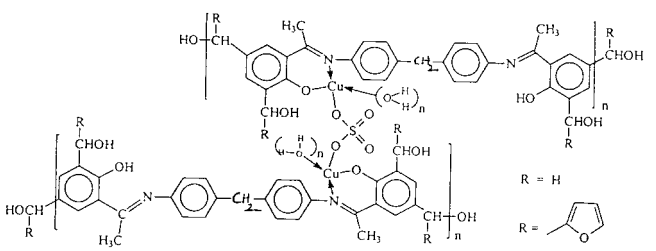

Figure 6 Intermolecular structure for *o*-HAP–DDM–HCHO–Cu(II) sulfate ion as a bridging bidentate ligand.

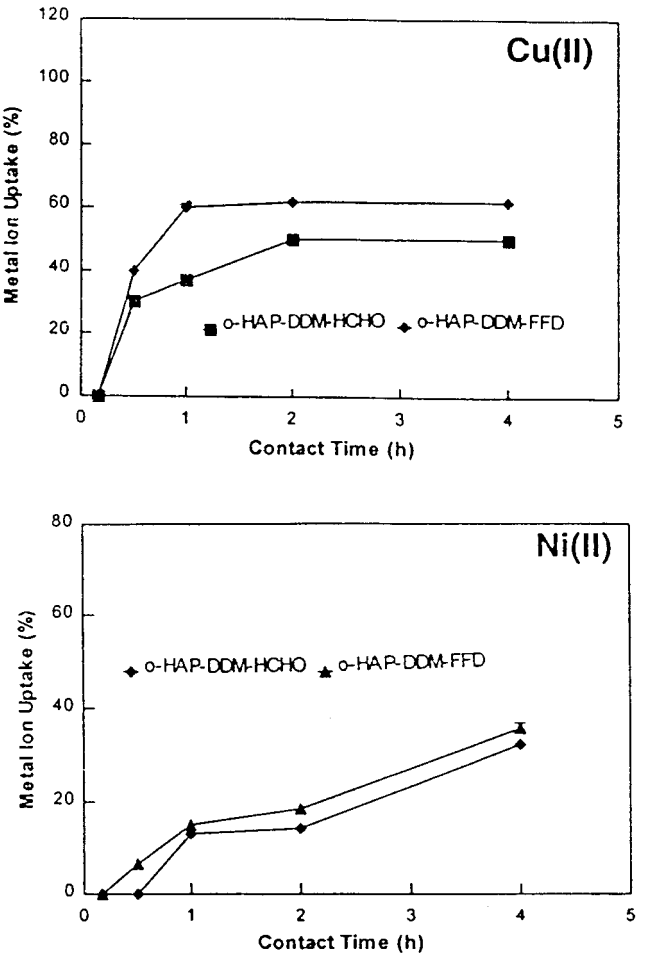

Figure 7 Effect of contact time on the adsorption of metal ions: [M(II)] = 2000 μg/10 mL; 500 μg/10 mL for *o*-HAP–DDM–HCHO and *o*-HAP–DDM–FFD; sorbent size, 100 mesh; quantity, 100 mg; and pH, natural.

Metal ion uptake studies

Effect of contact time

The saturation time for the metal uptake of the resins was obtained by plotting percentage of metal uptake versus contact time, while keeping the initial metal ion concentration (10 mL, 50 μg/mL) constant (Figure 7). In both the resins, the rate of adsorption of Cu(II) is higher than that of Ni(II). Several authors[33,34] have noted higher adsorption for Cu(II) compared with other metal ions. It is further noticed that the metal ion uptake percentage is higher for the furfuraldehyde-condensed resin than for the formaldehyde-condensed resin. The reason for this difference could be the fact that in the case of the furfuraldehyde-condensed resin, the presence of a furan ring in the furfural moiety presumably did not lead to efficient molecular packing. This reason is further supported by the ease of solubility of the resin in a number of solvents. Also, the presence of a furan ring oxygen atom was responsible for the higher percentage up-

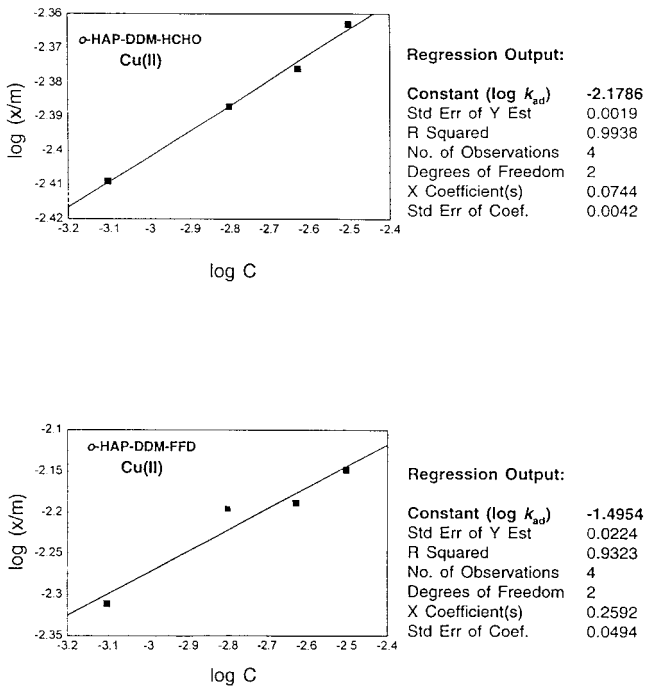

Figure 8 Evaluation of Freundlich adsorption isotherm paramters (k_{ad} and $1/n$) for adsorption of Ca(II) ion by the resins.

take of metal ion. However, in the case of the formaldehyde-condensed resin, the reason for the difference could be the fact that the various structural units in the resin matrix are connected through a —CH_2—group, leading to a rigid network structure. The low solubility of *o*-HAP–DDM–HCHO in various organic solvents supports the latter fact.

Often, insoluble chelating resins take up transition metal ions very slowly, because of the lower activity of the ligands placed inside the resin. The metal complexing nature of the resin depends not only on the nature of the ligand groups, but also the accessibility towards metal ions. Thus, steric hindrance by the polymeric matrix and the hydrophobic nature of the polymer ligands can limit the chelating reaction.[35]

Effect of metal ion concentration

The effect of metal ion concentration on the uptake behavior of the resins was studied in the concentration range 50–200 μg/mL (10 mL). Increasing metal ion concentration enhanced metal ion loading within the range of study. Beyond this ranges levelling effect was noticed because of the saturation of the available coordination sites of the resins. Tikhomirova et al.[36] observed a similar trend. Decreasing metal ion concentration slows down the reaction considerably. The adsorption coefficient, k_{ad}, of the resins for the adsorption of Cu(II) and Ni(II) was computed with the Freundlich adsorption isotherm (Figure 8):

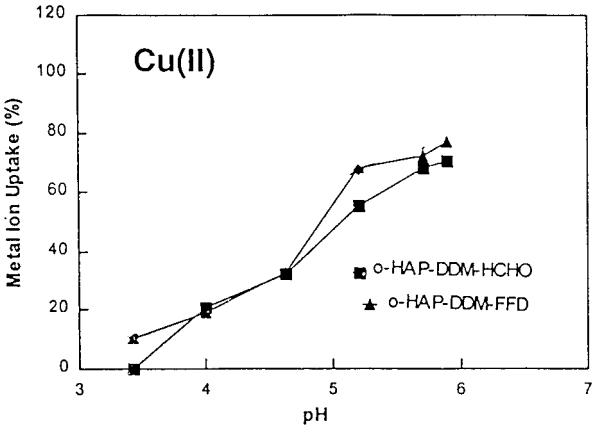

Figure 9 Effect of pH on the adsorption of Cu(II): [Cu(II)] (2000 μg/10 mL): 500 μg/10 mL for *o*-HAP–DDM–HCHO and *o*-HAP–DDM–FFD; resin quantity; 100 mg; sorbent size, 100 mesh; buffer, CH_3COONa/CH_3COOH; temperature, 30 °C; contact time, 24 h .

$$\log\left(\frac{x}{m}\right) = \log k_{ad} + \frac{1}{n}\ \log C \qquad (5)$$

where C is the initial concentration (mmol) of the metal ion, m is the weight (g) of the resin, x is the quantity (mmol) of the metal ion adsorbed by the resin, and n is a constant. The results are as follows: *o*-HAP–DDM–HCHO, for Cu(II) adsorption, $k_{ad} = 0.0066\ s^{-1}$, $n = 0.074$ and for Ni(II) adsorption, $k_{ad} = 0.0112\ s^{-1}$, $n = 0.199$; *o*-HAP–DDM–FFD, for Cu(II) adsorption, $k_{ad} = 0.0319\ s^{-1}$, $n = 0.259$ and for Ni(II) adsorption, $k_{ad} = 0.0190\ s^{-1}$ and $n = 0.261$. The high k_{ad} values indicate that the saturation time for adsorption of metal ion was attained quickly. Luo and coworkers[37] reported the adsorption constant for Mo^{6+} and W^{6+} and slow adsorption rate for metal ion was associated with low k_{ad} values.

TABLE IV
Effect of Added Salts on the Adsorption of Cu(II) Ion by the Resins[a]

Resin	M(II) uptake (%)			
	In the absence of added salt	In the presence added salt, M^{n+}		
		Na^+	K^+	Mg^{2+}
Cu(II)				
o-HAP-DDM-HCHO	49.6	47.24	48.5	47.94
o-HAP-DDM-FFD	62.36	61.08	62.04	60.62
Ni(II)				
o-HAP-DDM-HCHO	32.2	28.4	27.9	28.1
o-HAP-DDM-FFD	36.66	35.1	35.2	33.3

[a] Conditions: [M(II)]; 500 μg/10 mL; resin quantity, 100 mg; sorbent size, 100 mesh; temperature, 30°C; contact time, 24 h; [M^{n+}], 500 μg/10 mL; pH, natural; common anion, SO_4^{2-}.

TABLE V
Separation of Cu(II) from Ni(II) with Increasing Ni(II) Concentration at Fixed pH[a]

Resin	[M(II)], μg/10mL		Metal uptake (%)	
	Cu(II)	Ni(II)	Cu(II)	Ni(II)
o-HAP-DDM-HCHO	500	200	63.9	0
		400	67.8	0
		600	67.2	12.3
		800	65.3	14.3
o-HAP-DDM-FFD	500	200	80.3	0
		400	80.3	0
		600	78.3	13.3
		800	76.2	15.1

[a] Conditions: resin quantity, 100 mg: size, 100 mesh; pH, 5.89; temperature, 30°C; contact time, 24 h.

Effect of pH of the reaction medium

The effect of pH of the reaction medium on the extent of absorption of Cu^{2+} and Ni^{2+} was studied using buffers in the pH ranges 3.42–5.89 for Cu^{2+} and 3.42–8.8 for Ni^{2+}. An increase in pH beyond the range of study resulted in precipitation of metal ion as hydroxide. The metal ion uptake by the resins increased significantly with an increase in pH of the medium (Figure 9). This result was ascribed to the ease of coordination of the phenoxide ion compared with that of the phenolic O—H group at higher pH in addition to the enhanced basicity of the C═N nitrogen that was protonated in the acidic medium. Several workers[38] have reported enhanced adsorption of metal ions with an increase in the pH. The optimum pH of adsorption was 5.89 and 8.8, respectively, for Cu^{2+} and Ni^{2+}. The metal ion uptake percentage was reported to be higher in case of furfuraldehyde-condensed resin than that of formaldehyde-condensed resin. However, both resins showed higher affinity towards Cu^{2+} than Ni^{2+}. Suggi et al.[39] studied the chelating property of polystyene-based chelating resin containing oxime and dimethylamino functional groups and reported the highest capacity for Cu^{2+} at pH 6.0.

Effect of alkali and alkaline earth metal ions

To determine the interference of Na^+, K^+, and Mg^{2+} on the adsorption behavior of the resin, the two resins *o*-HAP–DDM–HCHO and *o*-HAP–DDM–FFD were treated with metal ions containing 50 μg/mL of Cu^{2+} and Ni^{2+}, and 50 μg/mL of Na^+, K^+, and Mg^{2+} (SO_4^{2-} as common anion) for 24 h at the natural pH of the solution. The added cations did not significantly affect the uptake of Cu^{2+} and Ni^{2+} ions by the resins (Table IV). Thus, the resin could be used to remove the Cu^{2+} ions from saline and nonsaline water that was rich in these cations. Dev and Rao[38b] also reported that the alkali and alkaline earth metals did not affect the uptake capacity of the resin towards Cu(II), Ni(II), and Co(II).

Adsorption behavior in the presence of both Cu(II) and Ni(II)

The metal ion uptake percentage of both *o*-HAP–DDM–HCHO and *o*-HAP–DDM–FFD resins towards Cu(II) and Ni(II) in a mixture was studied to determine the behavior of the resins under competitive conditions. The results are shown in Table V. The concentration of Ni(II) was varied while maintaining the concentration of Cu(II) and the pH of the medium at fixed values. At low Ni(II) concentration, the uptake percentage of Cu(II) remained nearly unaffected. With an increase in Ni(II) concentration, the uptake percentage of the Cu(II) decreased in both the resins. The extent of adsorption of Ni(II) was significantly lower than that of Cu(II). Dev and Rao[38a] employed N-hydroxyethylenediamine functionalized resins for effective separation of Cu(II) from Ni(II) and Co(II) from Cd(II). Further studies involving preconcentration and separation of some trace elements, like UO_2^{2+} and Mo(IV), in the presence of other anions and cations are in progress, and the results will be presented in our subsequent communications.

We thank the different Regional Sophisticated Instrumentation Centres located at Central Drug Research Institute, Lucknow; Punjab University, Chandigarh, IIT Mumbai, and IIT Chennai for providing analytical facilities. We also thank M/s Jagannath Computer Centre, Parlakhemundi, for providing a computer facility to carry out the work.

References

1. (a) Schmuckler, G. Talanta 1965, 12, 281; (b) Blasius, E.; Brozio, B. In Chelates in Analytical Chemistry, Vol. I; Flaschka, H. A.; Barnard, Jr, A. J., Eds.; Marcel Deckker: New York, 1967; p. 49; (c) Mayasova, G. V.; Savvin, S. B. Crit. Rev Anal. Chem 1986, 17, 1; (d) Kantipuly, C.; Katragadda, S.; Chow, A.; Gesser, H. D. Talanta 1990, 37, 491; (e) Biswas, M.; Mukherjee, A. Adv Poly Sci 1994, 115, 89; (f) Riley, J. P.; Taylor, D. Anal Chim Acta 1968, 40, 479; (g) Garg, B. S.; Sharma, R. K.; Bhojak, N.; Mittal, S. Microchem J 1999, 61, 94.
2. Parmer, J. S.; Patel, M. L.; Patel, M. N. Angew Makromol Chem 1981, 93, 1.
3. Zigon, M.; Sebenik, A.; Osredkar, U.; Vizovisek, I. Die Angew Makromol Chem 1987, 148, 127.
4. Zigon, M.; Sebenik, A.; Osredkar, U. Makromol Sci Chem 1988, A25(8), 942.
5. Moyers, E.; Fritz, J. S. Anal Chem 1977, 49(3), 418.
6. Dumont, N.; Tavre-Reguillon, A.; Dunjic, B.; Lemaire, M. Sep Sci Technol 1996, 31(7), 1001.
7. Samanta, S. K.; Mishra, B. 1995, Solv Exter Ion Exch 1995, 13(3), 575.
8. Sakaguchi, T.; Nakajima, A. Sep Sci Technol 1986, 21, 519.
9. Hodgklin, J. H.; Eilb, R. React Polym Ion Exch Sorbents 1985, 3, 83.
10. (a) Ueno, K.; Martell, A. E. J Phys Chem 1955, 59 998, and 1956, 60, 1270; (b) Okawa, H., et al. J Chem Soc Dalton Trans 1985, 54;

(c) Sinn, E., et al. Inorg Chem 1985, 24, 127; (d) Collins, T. H., et al. J Am Chem Soc 1986, 108 6593; (e) Che, C.- M; Cheng, W.- K. J Chem Soc, Chem Commun 1986 1443.
11. (a) Samal, S.; Das, R. R.; Sahoo, D.; Acharya, S. Polym Int 1997, 44, 41; (b) Samal, S.; Mohapatra, N. K.; Acharya, S.; Dev, R. K. React Polym 1999, 42, 37.
12. Bassett, J.; Denny, R. C.; Jeffery, G. H.; Mendham, J. Inorg Vogels Text Book of Quantative Analysis, 4th ed., Longman, Group: Harlow, U.K., 1978; pp. 156 and 747.
13. Updegraff, I. H.; Suen, T. J. Condensation with Formaldehyde In Schildknecht, C. E., Skeist, J., Eds.; Polymerization Processes, Chapter 14; Wiley-Interscience: New York, 1977.
14. Yang, C.-P.; Chen, W.-T. J Polym Sci, Part A: Polym Chem 1994, 32, 1101.
15. Chiriac, C.; Stille, J. K. Macromolecules 1977, 10, 710.
16. Bajpai, U. D. N.; Rai, S.; Bajpai, A. J Appl Polym Sci 1993, 48, 1241.
17. Silverstein, R. M.; Bassler, G. C.; Morrill, T. C. Spectrometric Identification of Organic Compounds, ed. 4; John Wiley: New York, 1981; Chapter 3, p. 130.
18. Chen, H.; Cronin, J. A.; Archer, R. D. Macormolecules 1994, 32, 1101.
19. Thamizharasi, S.; Reddy, A. V. R. Polymer 1992, 33, 2421.
20. Oriel, L.; Alonso, P. J.; Martineoz, J. I.; Pinol, M.; Serrano, J. L. Macromolecules 1994, 27, 1869.
21. Nakamato, K.; Fujita, J.; Tanaka, S.; Kobayashi, M. J Am Chem Soc 1957, 79, 4904.
22. Gatehouse, B. M.; Livingston, S. E.; Nyholm, R. S. J Chem Soc 1957, 4222.
23. Chiang, W.; Mej, W. Eur Poly J 1993, 29, 1047.
24. Chen, H.; Cronin, J. A.; Archer, R. D. Macromolecules 1994, 27, 2174.
25. Kizilcan, N.; Akar, A. J Appl Polym Sci 1998, 70, 65.
26. Chamberlain, N. F. The Practice of NMR Spectroscopy; Plenum New York, 1974; p. 302.
27. Dimitrov, V. I.; Novakoy, P.; Miloshev, S. Polymer 1992, 33(7), 1543.
28. Coats, A. W.; Redfern, J. P. J Polym Sci, Polym Lett 1965, 3, 921.
29. Van Krevelen, D. W.; Van Heerden, C.; Humfjens, F. J. Fuel 1951, 30, 253.
30. Broido, A. J Polym Sci, Polym Lett 1969, A-2 7, 1761.
31. Biswas, M.; Mukherjee, A. J Appl Polym Sci 1992, 46, 1453; Biswas, M.; Moitra, A. J Appl Polym Sci 1989, 38, 1243.
32. Yagci, Y.; Denizligil, S.; Bicak, N.; Atav, T. Angew Makromol Chem 1992, 195, 89.
33. Mendez, R.; Pillai, V. N. S. Analyst 1990, 11, 213.
34. Verweij, P. D.; Reedijk, J. Eur Polym J 1993, 29(12), 1603.
35. Lezzi, A.; Cobianco, S.; Roggero, A. J Polym Sci, Part A 1994, 32, 1877.
36. Tikhkomirova, T. I.; Fadeeva, V. I.; Kubryavtsev, G. V.; Nestorenko, P. N.; Ivanov, V. M.; Savitchey, A. T.; Smirnova, N. S. Talanta 1991, 38(3), 267.
37. Lug, X.-Y.; Su, Z.-X.; Gao, W.-Y.; Zhom, G.-Y.; Chang, X.-J. Analyst 1992, 117, 145.
38. (a) Dev, K.; Rao, G. N. Analyst 1990, 120, 2509; (b) Dev, K.; Rao, G. N. Talanta 1996, 43, 451.
39. Sugii, A.; Ogawa, N.; Hashizume, H. Talanta, 1979, 26, 189.